

Ancient deuterostome origins of vertebrate brain signalling centres

Ariel M. Pani^{1,2}, Erin E. Mullarkey^{3*}, Jochanan Aronowicz^{4*}, Stavroula Assimacopoulos⁵, Elizabeth A. Grove^{3,4,5} & Christopher J. Lowe^{1,2,4}

Neuroectodermal signalling centres induce and pattern many novel vertebrate brain structures but are absent, or divergent, in invertebrate chordates. This has led to the idea that signalling-centre genetic programs were first assembled in stem vertebrates and potentially drove morphological innovations of the brain. However, this scenario presumes that extant cephalochordates accurately represent ancestral chordate characters, which has not been tested using close chordate outgroups. Here we report that genetic programs homologous to three vertebrate signalling centres—the anterior neural ridge, zona limitans intrathalamica and isthmic organizer—are present in the hemichordate *Saccoglossus kowalevskii*. *Fgf8/17/18* (a single gene homologous to vertebrate *Fgf8*, *Fgf17* and *Fgf18*), *sfrp1/5*, *hh* and *wnt1* are expressed in vertebrate-like arrangements in hemichordate ectoderm, and homologous genetic mechanisms regulate ectodermal patterning in both animals. We propose that these genetic programs were components of an unexpectedly complex, ancient genetic regulatory scaffold for deuterostome body patterning that degenerated in amphioxus and ascidians, but was retained to pattern divergent structures in hemichordates and vertebrates.

During vertebrate development, the brain arises from coarsely patterned planar neuroectoderm through successive refinement of regional identities, resulting after morphogenesis and growth in a complex structure composed of highly specialized areas^{1–3}. In contrast, invertebrate chordates have relatively simple nervous systems that lack unambiguous homologues of many vertebrate brain regions^{4–6}. These clear disparities in nervous system complexity indicate that key innovations in patterning mechanisms have attended the evolution of the vertebrate brain from a simpler central nervous system (CNS). However, attempts to identify the presumed genetic regulatory novelties have been mainly inconclusive, and comparative studies have mostly revealed similarities, rather than differences, in the early transcriptional architectures of diverse bilaterian nervous systems^{7–12}. Notable exceptions are CNS signalling centres, which have emerged as strong candidates for vertebrate genetic regulatory novelties involved in early vertebrate brain evolution^{8–10}. These centres act as secondary organizers that mediate regional patterning in the CNS and are often necessary and sufficient for the establishment of vertebrate-specific brain structures^{1–3,13–18}.

The anterior neural ridge (ANR), zona limitans intrathalamica (ZLI) and isthmic organizer (IsO) are the three primary signalling centres that direct anteroposterior patterning in the vertebrate anterior neural plate and then later in the developing brain^{1–3}. Homologous signalling centres and their molecular signatures are absent, or divergent, in amphioxus and ascidians^{8–10,19–25}, consistent with the idea that they are vertebrate novelties whose origins could have driven CNS innovations in stem vertebrates^{8–10}. However, this idea depends on amphioxus adequately representing ancestral states for chordate developmental genetic characters, and does not account for the possibility of secondary losses in cephalochordates. Here we present developmental data from the hemichordate *S. kowalevskii* to test an alternative scenario for signalling-centre origins; namely, that ANR, ZLI and IsO genetic programs pre-date chordate origins and

were secondarily simplified or lost along the lineages leading to the invertebrate chordates.

Hemichordates are a deuterostome phylum closely related to chordates²⁶ and are a promising outgroup for investigating chordate evolution. Previous studies established that despite substantial body-plan divergence between the two groups, hemichordates and vertebrates share a broadly conserved transcriptional regulatory architecture during early body patterning^{7,27–29}, which is demonstrated by the close similarities in spatial arrangements of expression domains of many transcription factors that are involved in early bilaterian anteroposterior patterning. This combination of morphological divergence and developmental genetic similarity makes hemichordates an informative outgroup for testing the proposed coupling of vertebrate morphological and developmental genetic innovations. Here, we present descriptive and functional evidence that genetic programs homologous to the ANR, ZLI and IsO are present in *S. kowalevskii*, indicating that they were elements of an ancient developmental genetic toolkit for deuterostome body patterning that were subsequently modified and elaborated in stem vertebrates to regulate brain development.

An ANR-like regulatory program in hemichordates

The ANR is located in the anterior neural plate of vertebrates and is a source of fibroblast growth factors (FGFs) and secreted frizzled-related proteins (SFRPs), which establish and pattern the telencephalon^{1,2,15,16,30,31}. Topologically consistent with vertebrate CNS expression domains, *sfrp1/5* and *fgf8/17/18* are expressed in *S. kowalevskii* anterior proboscis ectoderm (Fig. 1a–d). In vertebrates, FGFs and antagonists of the Wnt pathway mediate ANR function and telencephalon patterning^{15,16,30–32}. In mice, conditional *Fgfr1*, *Fgfr2* and *Fgfr3* knockout abolishes the telencephalon¹⁶, whereas *Fgf8* mutants have a posteriorized neocortex³³. Similarly, treating *S. kowalevskii* embryos with the FGF receptor inhibitor SU5402 (ref. 34) from late gastrula through to

¹Committee on Evolutionary Biology, The University of Chicago, 1025 East 57th Street, Chicago, Illinois 60637, USA. ²Hopkins Marine Station, Department of Biology, Stanford University, 120 Oceanview Boulevard, Pacific Grove, California 93950, USA. ³Committee on Neurobiology, The University of Chicago, 947 East 58th Street, Chicago, Illinois 60637, USA. ⁴Department of Organismal Biology and Anatomy, The University of Chicago, 1027 East 57th Street, Chicago, Illinois 60637, USA. ⁵Department of Neurobiology, The University of Chicago, 947 East 58th Street, Chicago, Illinois 60637, USA.

*These authors contributed equally to this work.

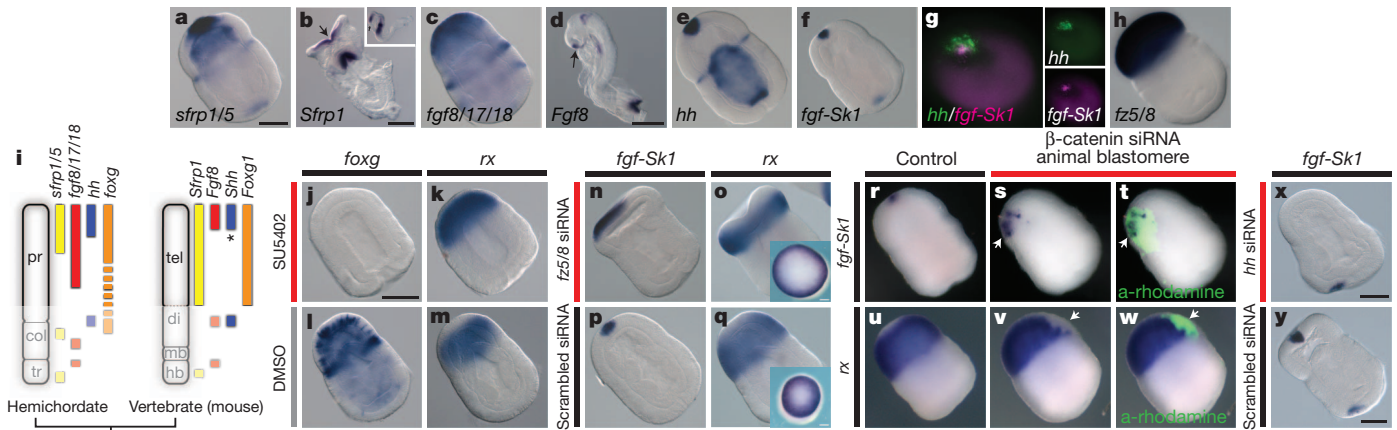


Figure 1 | An ANR-like signalling centre in *S. kowalevskii*. **a–h**, *S. kowalevskii* and mouse *in situ* hybridizations for markers of ANR and telencephalon. *S. kowalevskii* embryos are at the double-groove stage (36 h), and are shown in dorsal view with the anterior (proboscis) to the top left of the image, except where noted. Embryos are optically cleared except in **o**, **q** (insets) and **r–w**. Mouse embryos are at approximately embryonic day 8.5. **a**, *S. kowalevskii* *sfrp1/5* expression. **b**, Frontal view of mouse *Sfrp1* expression; arrowhead denotes ANR. Inset shows lateral view. **c**, *S. kowalevskii* *fgf8/17/18* expression. **d**, Mouse *Fgf8* expression; arrowhead denotes ANR. **e**, *S. kowalevskii* *hh* expression. **f**, *S. kowalevskii* *fgf-Sk1* expression. **g**, Frontal view of double FISH for *hh* and *fgf-Sk1*. **h**, *fz5/8* expression. **i**, Anteroposterior expression topologies in *S. kowalevskii* and mouse embryos. Anterior to top. Asterisk indicates *Shh* is expressed in the medial ganglionic eminence, near the ANR. **j–k**, *foxg* (**j**) and *rx* (**k**) expression in embryos treated with SU5402. **l**, *foxg* (**l**) and *rx*

double-groove stages (28–36 h) eliminated the morphological boundary between the proboscis and collar, and resulted in altered gene expression domains, indicating loss and/or posteriorization of anterior proboscis (Fig. 1j–m). Expression of *foxg*, the *S. kowalevskii* homologue of the telencephalon marker *foxg1*, was completely eliminated (Fig. 1j, l), whereas *rx*, which is normally excluded from the anterior proboscis, was expressed up to the anterior limit of the embryo (Fig. 1k, m).

Wnt antagonists expressed in the ANR and/or telencephalon are also critical for forebrain development in vertebrates^{2,15,35}. To explore potential similarities in Wnt functions between the telencephalon and proboscis, we first suppressed Wnt activity in the developing proboscis by using short interfering RNA (siRNA) microinjections to knock down the Wnt receptor *frizzled 5/8*, which is expressed with a sharp boundary at the proboscis base (Fig. 1h). *Fz5/8* siRNA expanded apical identity at the expense of the posterior proboscis, as demonstrated by expansion of the apical marker *fgf-Sk1* (Fig. 1n, p) and contraction of *rx* expression to a more posterior domain (Fig. 1o, q). Embryos that were injected with a scrambled control siRNA were indistinguishable from wild-type embryos (Fig. 1p, q), and the effects of *fz5/8* knockdown were limited to its endogenous expression domain (Supplementary Fig. 1). Second, we suppressed Wnt signalling in small patches of proboscis ectoderm by injecting β -catenin siRNA into single animal blastomeres at early cleavage stages. β -catenin-deficient clones in the posterior proboscis ectoderm expressed the apical marker *fgf-Sk1* (Fig. 1r–t), but not the more posterior proboscis marker *rx* (Fig. 1u–w), which indicates a transformation of posterior to apical fate in the absence of local Wnt signalling.

Although not a genetic component of the ANR itself, *sonic hedgehog* (*Shh*) is expressed in the nearby medial ganglionic eminence^{1,36} (see Fig. 2c, d) and interacts with FGFs to regulate telencephalon patterning³⁷. The apical *S. kowalevskii* proboscis ectoderm expresses *hedgehog* (*hh*; a homologue of *Shh*) (Fig. 1e) in a domain that partially overlaps *fgf-Sk1* (Fig. 1f), with *hh* more broadly expressed dorsally and laterally (Fig. 1g). Embryos injected with *hh* siRNA lacked apical *fgf-Sk1* expression (Fig. 1x, y) indicating that *hh* at least partially regulates anterior FGF signalling and apical–ventral patterning. This finding

raises the possibility that an anterior signalling domain including FGFs, Wnt antagonists and *hh* was present in stem deuterostomes and was spatially partitioned during vertebrate evolution.

(m) expression in embryos treated with DMSO. **n**, Expanded apical *fgf-Sk1* expression in an embryo injected with *fz5/8* siRNA. **o**, Retracted *rx* expression in an embryo injected with *fz5/8* siRNA. **p**, *fgf-Sk1* expression in a siRNA control embryo. **q**, *rx* expression in a siRNA control embryo. Insets in **o**, **q** show frontal views of uncleared embryos. **r**, Wild-type *fgf-Sk1* expression. **s**, *fgf-Sk1* expression in descendants of a blastomere injected with β -catenin siRNA. **t**, Merged darkfield and fluorescence images showing clonal descendants of the injected cell (green). **u**, Wild-type *rx* expression. **v**, *rx* is not expressed in descendants of a blastomere injected with β -catenin siRNA. **w**, Merged darkfield and fluorescence images showing the location of the β -catenin-deficient clone (green). **x**, *fgf-Sk1* expression in an embryo injected with *hh* siRNA. **y**, *fgf-Sk1* expression in a siRNA control embryo. Scale bars, 100 μ m in *S. kowalevskii*, and 200 μ m (**b**) and 500 μ m (**d**) in mice. col, collar; di, diencephalon; hb, hindbrain; mb, midbrain; pr, proboscis; tel, telencephalon; tr, trunk.

raises the possibility that an anterior signalling domain including FGFs, Wnt antagonists and *hh* was present in stem deuterostomes and was spatially partitioned during vertebrate evolution.

A ZLI-like regulatory program in hemichordates

The ZLI is located in the vertebrate diencephalon and specifies the flanking prethalamus and thalamus^{1,17,18,23}. The molecular signature of the ZLI is a narrow, transverse domain of *Shh* expression (Fig. 2c, d) that patterns the mid-diencephalon along its anteroposterior axis^{17,18,23}. A homologous *hh* expression domain is absent in invertebrate chordates, supporting the idea that the ZLI is a vertebrate genetic innovation, possibly associated with forebrain origins^{10,21–23}. Notably, we found that *S. kowalevskii* *hh* is expressed in a circumferential ectodermal band at the proboscis–collar boundary (Fig. 2a) in a transcriptional context of expression domains that is similar to the vertebrate forebrain⁷. Expression of the Hh receptor *ptch* in an overlapping but broader domain than *hh* itself, indicates that *hh* signals to adjacent ectoderm (Fig. 2b) similar to the ZLI (Fig. 2e, f). The proboscis–collar boundary region also expresses *fng*, *otx*, *wnt8* (Fig. 2g–m, v) and *six3* (ref. 7) in spatial arrangements that are characteristic of the mid-diencephalon and ZLI. In vertebrates, *lfng* is expressed broadly in the diencephalon except for the ZLI (ref. 38), whereas *Wnt8b* and *Otx* genes mark the ZLI itself in a combinatorial pattern that is unique to this region¹⁸ (Fig. 2i, j, m). *S. kowalevskii* *hh* is also expressed in a *fng*-negative, *otx*- and *wnt8*-positive territory posterior to *six3* (ref. 7) (Fig. 2g, h, k, l, v). Notably, the hemichordate homologues of *irx* and *fezf*, which abut at the ZLI and are expressed in anterior abutting domains in *Drosophila* and amphioxus (ref. 10), show divergent expression patterns in *S. kowalevskii* (Supplementary Fig. 2), indicating secondary modification in hemichordates. In vertebrates, *Otx* genes are expressed in restricted domains in the mid-diencephalon at the stage when the ZLI forms (Fig. 2i, j), and *otx11* and *otx2* knockdown eliminates *shh* expression at the zebrafish ZLI³⁹. Similarly, in *S. kowalevskii*, *hh* and *otx* are co-expressed in the presumptive proboscis–collar boundary ectoderm shortly after gastrulation (Fig. 2k), and *otx* siRNA knockdown reduced *hh* expression at the proboscis–collar boundary (Fig. 2w, x).

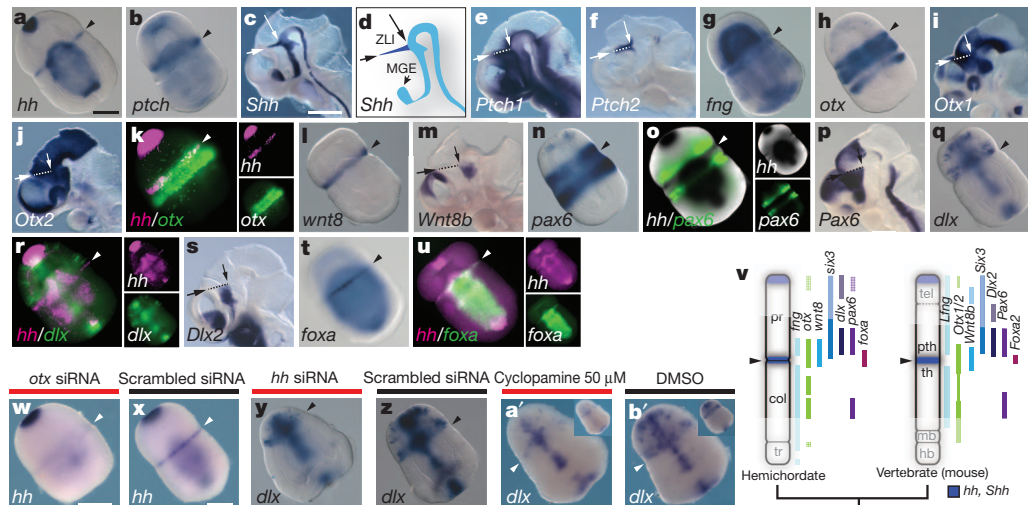


Figure 2 | A ZLI-like signalling centre in *S. kowalevskii*. **a–u**, *In situ* hybridizations for *S. kowalevskii* and mouse homologues of ZLI and diencephalon markers. Arrowheads mark the proboscis–collar boundary in *S. kowalevskii*. Mouse images show hemisected heads at embryonic day 10.5, and dashed lines indicate the ZLI, with arrows denoting its extent. **a**, *S. kowalevskii* *hh* expression. **b**, *S. kowalevskii* *ptch* expression (see Supplementary Fig. 3). **c**, mouse *Shh* expression. **d**, Diagram of *Shh* expression showing ZLI in dark blue. **e**, Mouse *Ptch1* expression. **f**, Mouse *Ptch2* expression. **g**, *S. kowalevskii* *fng* expression. **h**, *S. kowalevskii* *otx* expression. **i**, Mouse *Otx1* expression. **j**, Mouse *Otx2* expression. **k**, *hh* (magenta) and *otx* (green) are co-expressed at the presumptive proboscis–collar boundary. **l**, *S. kowalevskii* *wnt8* expression. **m**, Mouse *Wnt8b* expression. **n**, *S. kowalevskii* *pax6* expression. **o**, Double *in situ* hybridization showing *pax6* expression (fluorescence, green) anterior to *hh*

(colorimetric, black). **p**, Mouse *Pax6* expression. **q**, *S. kowalevskii* *dlx* expression. **r**, Double FISH showing *dlx* expression (green) in the proboscis base anterior to *hh* (magenta). **s**, Mouse *Dlx2* expression. **t**, *S. kowalevskii* *foxa* expression. **u**, Double FISH showing *foxa* (green) and *hh* (magenta) expression. **v**, Diagram of anteroposterior expression topologies of ZLI and forebrain marker homologues in *S. kowalevskii* and mice. *Six3* expression based on previous data⁷. Anterior to top. **w**, **x**, *otx* siRNA downregulates *hh* expression at the proboscis–collar boundary (**w**) relative to a control siRNA (**x**). **y**, **z**, *hh* siRNA reduces *dlx* expression in the proboscis base (**y**) relative to a scrambled siRNA (**z**). **a'**, **b'**, cyclopamine treatment reduces *dlx* expression in the proboscis base (**a'**) relative to a control embryo treated with DMSO (**b'**). Insets show ventral views. Scale bars, 100 μ m in *S. kowalevskii* embryos, 1 mm in mice. MGE, medial ganglionic eminence; pth, prethalamus; th, thalamus.

Hemichordate homologues of diencephalic markers regulated by *Shh* at the vertebrate ZLI are also expressed in similar topological arrangements at the *S. kowalevskii* proboscis–collar boundary. In vertebrates, *Pax6* and *Dlx2* are expressed anterior to the ZLI in the prethalamus (Fig. 2p, s), where their expression requires *Shh*^{17,18}. Similarly, *S. kowalevskii* *pax6* and *dlx* are expressed anterior to *hh* at the proboscis base (Fig. 2n, o, q, r, v). In vertebrates, *Foxa2* is expressed in the ZLI itself¹⁷, and in *S. kowalevskii*, *foxa* is expressed at the proboscis–collar boundary (Fig. 2t, u). Targeting *hh* function in *S. kowalevskii* by injecting *hh* siRNA downregulated *dlx* at the proboscis–collar boundary (Fig. 2y, z). However, these embryos had other strong defects in anteroposterior and dorsoventral patterning, probably owing to *hh* having additional roles that complicated the assessment of *hh* function at the proboscis–collar boundary (Supplementary Fig. 3). To reduce early pleiotropic effects, we treated embryos with the Hh signalling inhibitor cyclopamine⁴⁰ from the end of gastrulation through double-groove stage. Treating embryos with 50 μ M cyclopamine downregulated *dlx* at the proboscis–collar boundary with limited effects on midline expression and general morphology (Fig. 2a', b'), suggesting that Hh signalling from the proboscis–collar boundary regulates *dlx*. The prominent similarities in expression of ZLI marker homologues in *S. kowalevskii* and vertebrates, and the conserved functions for *otx* and *hh*, suggest that an ancestral signalling centre homologous to the ZLI was present in early deuterostomes.

An ISO-like regulatory program in hemichordates

The ISO is located at the midbrain–hindbrain boundary (MHB) and is defined molecularly by abutting domains of FGF8 and WNT1, which induce and pattern adjacent neural structures^{1,3,13,14,42}. The search for a pre-vertebrate ISO has focused on expression patterns of these ligands along with orthologues of the transcription factors *otx*, *gbx*, *en* and *pax2/5/8*, whose combinatorial expression patterns in vertebrates define a molecular territory unique to the MHB (Fig. 3b, d, g, i, m, p–r). In amphioxus, CNS expression of *fgf8/17/18* is restricted to the

anterior cerebral vesicle^{19,24}, and *wnt1* is not expressed in the CNS²⁵. In *Ciona intestinalis*, *fgf8/17/18* is expressed in the larval visceral ganglion where it regulates *en* and *pax2/5/8* to delineate the sensory vesicle and neck regions²⁰, suggesting that at least a partial ISO-like signalling centre pre-dates vertebrates. However, *wnt1* is absent in the *C. intestinalis* genome, making it difficult to infer the full extent of this ancestral centre. In *Drosophila melanogaster*, *otx* and *gbx* orthologues are expressed in patterns similar to those at the MHB, but the absence of compelling similarities in the expression of *fgf8/17/18*-related genes, and repeated expression of *wnt1* and *en* at parasegmental boundaries¹² weakens the idea of homology with the vertebrate ISO. To assess the presence of an ISO-like region in hemichordates, we investigated expression patterns for *S. kowalevskii* homologues of vertebrate MHB markers (Fig. 3a–t). We found that at double-groove stage (36 h), *fgf8/17/18* and *wnt1* are expressed in adjacent ectodermal bands in the anterior trunk with *wnt1* expressed anterior to *fgf8/17/18* (Fig. 3a, c, e); a topology similar to the vertebrate ISO (Fig. 3b, d). In vertebrates, abutting domains of *otx* and *gbx* genes position the ISO (ref. 3), and opposing *otx* and *gbx* domains are also found in protostomes¹² and amphioxus^{8,9}, indicating that this pattern is ancestral to bilaterians. A reassessment of *otx* and *gbx* expression patterns in *S. kowalevskii*⁷ revealed that they are also expressed in adjacent domains at the collar–trunk coelom boundary, with *gbx* expressed in the ectoderm between the most posterior *otx* domains (Fig. 3f, h, j). However, the spatial arrangements of *otx* and *wnt1*, and *gbx* and *fgf8/17/18*, are reversed in *S. kowalevskii* and vertebrates (Fig. 3t) indicating that divergent mechanisms position homologous ISO-like regions in these groups. In vertebrates, *pax2*, *pax5* and *pax8*, and *en1* and *en2* are co-expressed at the MHB (Fig. 3m, p–r). However, expression of *pax2/5/8* and *en* does not overlap in *S. kowalevskii* (Fig. 3n, o) or invertebrate chordates^{9,20}, which suggests that regulation of *en* genes by *pax2/5/8* genes is a novel feature of vertebrate development. Beyond similarities in expression of signalling molecules and transcription factors, we found that the catecholaminergic neuron marker tyrosine hydroxylase is co-expressed

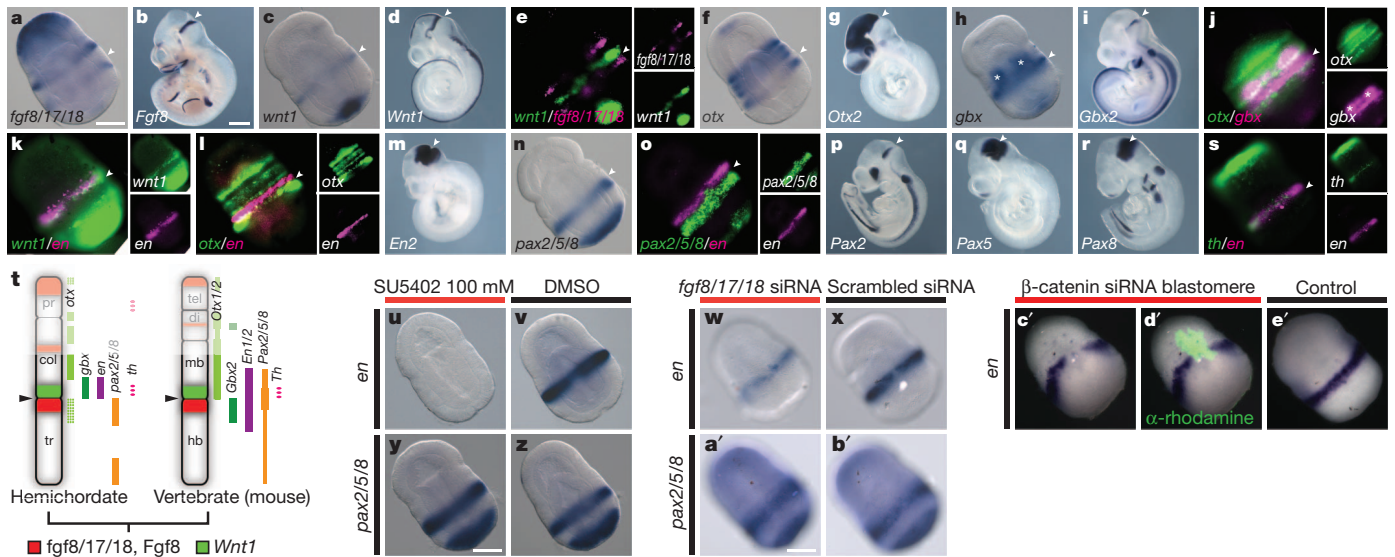


Figure 3 | An IsO-like signalling centre in *S. kowalevskii*. a–s, *In situ* hybridizations for *S. kowalevskii* and mouse homologues of MHB markers. Arrowheads mark the *S. kowalevskii* collar–trunk coelom boundary and the mouse IsO. a, *S. kowalevskii* *fgf8/17/18* expression. b, Mouse *Fgf8* expression. c, *S. kowalevskii* *wnt1* expression. d, Mouse *Wnt1* expression. e, Double FISH showing *S. kowalevskii* *wnt1* (green) expressed directly anterior to *fgf8/17/18* (magenta). f, *S. kowalevskii* *otx* expression. g, Mouse *Otx2* expression. h, *S. kowalevskii* *gbx* expression. Asterisks denote endodermal domains. i, Mouse *Gbx2* expression. j, Double FISH for *S. kowalevskii* *otx* (green) and *gbx* (magenta). k, Double FISH for *S. kowalevskii* *wnt1* (green) and *en* (magenta). l, Double FISH for *S. kowalevskii* *en* and *otx*. m, Mouse *En2* expression. n, *S. kowalevskii* *pax2/5/8* expression. o, Double FISH showing *S. kowalevskii* *pax2/5/8* and *en* expression. p–r, Expression of mouse *Pax2* (p), *Pax5* (q) and *Pax8* (r). s, Double FISH for *S. kowalevskii* tyrosine hydroxylase (green) and *en* (magenta). t, Summary of anteroposterior expression topologies in hemichordates and mice. Anterior to top. u, *en* expression is reduced in an embryo that has been treated with SU5402. v, *en* expression in a DMSO-treated control embryo. w, *en* expression in an embryo injected with *fgf8/17/18* siRNA. x, *en* expression in an embryo injected with a control siRNA. y, *pax2/5/8* expression in an embryo treated with SU5402. z, *pax2/5/8* expression in a DMSO-treated control embryo. a', *pax2/5/8* expression in an embryo injected with *fgf8/17/18* siRNA. b', *pax2/5/8* expression in an embryo injected with a control siRNA. c', *en* is not expressed in descendants of a blastomere injected with β -catenin siRNA. d', Merged darkfield and fluorescence images showing the location of the β -catenin-deficient clone (green). e', Wild-type *en* expression. Scale bars, 100 μ m in *S. kowalevskii* embryos; 1 mm in mice.

with *en* in the *S. kowalevskii* posterior collar (Fig. 3s) similar to vertebrates⁴¹, raising the possibility that this neuronal population is homologous to vertebrate midbrain dopaminergic neurons.

Functional assays further support the deep deuterostome ancestry of a MHB-like genetic module. In vertebrates, *fgf8* mediates the organizing abilities of the IsO and maintains expression of other MHB markers^{1,3,13,14}. To assess similar requirements for FGFs in hemichordates, we first treated embryos with 100 μ M SU5402 at the end of gastrulation to suppress FGF signalling without perturbing earlier patterning events. Expression of *en* was strongly reduced in SU5402-treated embryos (Fig. 3u, v), whereas *pax2/5/8* was unaffected (Fig. 3y, z), compared to control embryos treated with dimethylsulphoxide (DMSO). To test specifically for a role of *fgf8/17/18* in regulating collar–trunk patterning, we injected fertilized oocytes with *fgf8/17/18* siRNA. Knockdown of *fgf8/17/18* reduced *en* expression (Fig. 3w, x) but had no effect on *pax2/5/8* expression (Fig. 3a', b') relative to embryos injected with a scrambled control siRNA. The absence of any effect on *pax2/5/8* expression in these experiments highlights differences in gene regulation downstream of *fgf8/17/18* homologues between hemichordates and chordates^{3,20}.

In vertebrates, *Wnt1* is required to maintain expression of *en* genes at the MHB^{3,42}. To assess local Wnt functions at the *S. kowalevskii* collar–trunk boundary, we injected single blastomeres with β -catenin siRNA at early cleavage stages to suppress Wnt signalling in small patches of collar–trunk ectoderm. Clonal descendants of injected blastomeres failed to express *en* (Fig. 3c'–e'), suggesting a similar role for Wnts in regulating *en* genes at the MHB and collar–trunk boundary.

Discussion

Extensive similarities in expression patterns of signalling-centre markers and conserved functions for FGF, Wnt and Hh signals in *S. kowalevskii* and vertebrates provide compelling evidence that signalling centres

homologous to the ANR, ZLI and IsO were parts of an ancient genetic regulatory scaffold that pre-date the morphological innovations of vertebrates (Fig. 4). Therefore, assembly of these genetic networks did not trigger morphological novelties of the brain. Instead, early vertebrate brain evolution involved modifying and elaborating ancestral signalling centres to pattern novel structures within a highly conserved gene regulatory framework for anteroposterior ectodermal patterning⁷.

Widespread losses of signalling-centre components in invertebrate chordates and the unresolved nature of the ancestral deuterostome nervous system present a challenge for inferring when the ANR, ZLI and IsO genetic circuits were first deployed to regulate CNS patterning specifically, and to what extent these integrations could have been associated with origins of vertebrate novelties. In *S. kowalevskii*, signalling-centre programs are deployed at stages when the nervous system is still circumferentially organized⁷ and in body regions that have been described as containing components of the adult peripheral, rather than central, nervous system in the hemichordate *Ptychodera flava*⁴³. Notably, similar to their roles in the vertebrate brain, the ZLI and IsO-like signalling centres are located at morphological boundaries in *S. kowalevskii*, suggesting ancient roles in demarcating ectodermal divisions. We propose that rather than having evolved for CNS patterning, the most ancient role for signalling centres was in general body plan regionalization.

This work also highlights that basal chordates have not retained all ancestral chordate characters and have undergone substantial independent evolutionary changes. This is generally accepted for urochordates, but based on available data, cephalochordates are often considered to be the most informative extant group for reconstructing ancestral chordate characters^{8,9,24}. Our data provide clear evidence that secondary losses of complex developmental mechanisms have occurred in cephalochordates, and that overlooking this possibility

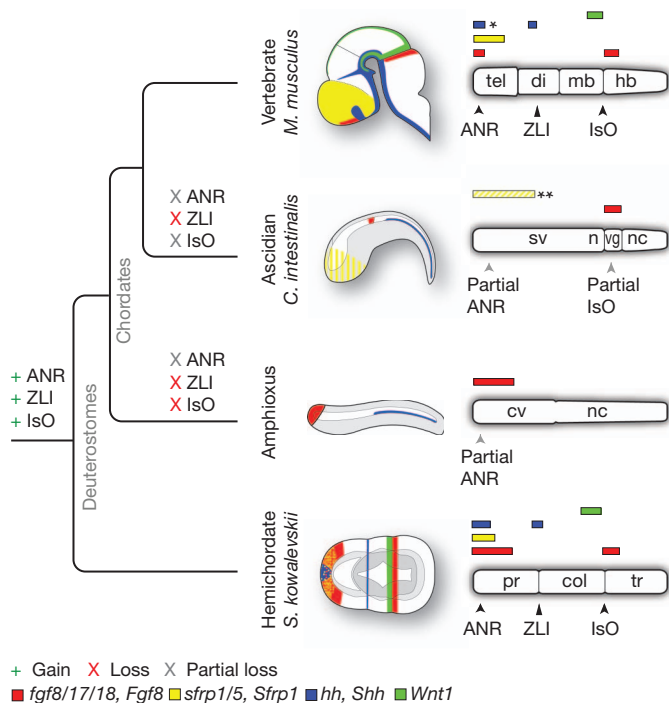


Figure 4 | Evolutionary gain and loss of ANR, ZLI and IsO-like genetic programs. Schematic diagrams depicting the expression of *Fgf8*, *Sfrp1*, *Shh* and *Wnt1* homologues in the mouse brain and ectoderm of *C. intestinalis*, amphioxus and *S. kowalevskii*. Embryos are oriented with their anterior side to the left of the image and their dorsal side to top. Bar diagrams are oriented with the anterior side to the left of the image. Diagrams depict only expression domains that are related to signalling components of vertebrate CNS signalling centres. cv, cerebral vesicle; n, neck; nc, nerve cord; sv, sensory vesicle; vg, visceral ganglion. Diagrams are not to scale. Single asterisk indicates that *Shh* is expressed in the medial ganglionic eminence, near the ANR. Double asterisk indicates that *sfrp1/5* is expressed in the *C. intestinalis* anterior ectoderm from the 64-cell stage up to neurulation but is then downregulated in the anterior ectoderm and CNS (shown as yellow stripes).

can inflate the numbers of putative vertebrate novelties. Although divergence of ANR, ZLI and IsO-like genetic programs in extant invertebrate chordate lineages may have been associated with the loss or modification of anterior ectodermal structures of the CNS and head, this is difficult to test. On the basis of these new observations, re-analysis of early chordate fossils that accommodates scenarios of greater anterior complexity in stem chordates may be informative. However, in the absence of additional fossil data, predictions of the morphological consequences of developmental genetic losses based on molecular data alone are unreliable.

This study provides a compelling example of the challenges associated with identifying key developmental genetic innovations responsible for morphological innovations at macroevolutionary scales. The unexpected presence of ANR, ZLI and IsO-like programs in *S. kowalevskii* highlights that basing outgroup choice solely on morphological criteria can lead to erroneous conclusions about links between morphological and developmental genetic characters: although by almost all morphological criteria amphioxus shares more similarities with vertebrates than do hemichordates, our data support the hypothesis that in certain cases hemichordates will be a more informative group than basal chordates for reconstructing stem chordate characters and understanding the origins of vertebrate developmental genetic processes. Additional data from protostomes, especially lophotrochozoans, will be required to assess whether the ANR, ZLI and IsO genetic programs are unique deuterostome features or have even deeper bilaterian origins.

Our findings highlight the importance of broad phylogenetic sampling, including morphologically divergent outgroups, to identify

gene regulatory innovations responsible for evolutionary changes in body plans. With growing use of novel model organisms, it seems that secondary losses of complex developmental regulatory characters may occur commonly^{44–46}, with consequences for morphological evolution that are still poorly understood. Conversely, the presence of complex developmental modules that regulate morphologically disparate structures in distantly related lineages suggests a loose coupling between morphological and gene regulatory evolution over macroevolutionary timescales, and highlights the difficulties of reconstructing ancestral morphological characters from molecular genetic data.

METHODS SUMMARY

Gravid *S. kowalevskii* were collected at Waquoit Bay National Estuarine Research Reserve near Woods Hole, Massachusetts, and maintained at the Marine Biological Laboratory, Woods Hole. Spawning and embryo rearing was carried out using established techniques⁷. For SU5402 and cyclopamine treatments, embryos were raised either in inhibitor, or in an equivalent concentration of DMSO, diluted in 0.2 μ m-filtered sea water. siRNA microinjections were performed as described previously^{27,29} using calcein or lysinated 10,000 molecular weight (MW) tetramethylrhodamine dextran tracers. Descendants of injected blastomeres were detected by anti-tetramethylrhodamine immunofluorescence. siRNA sequences are provided in Supplementary Table 1. Procedures involving mice (*Mus musculus*) were performed under a protocol approved by the University of Chicago Institutional Animal Care and Use Committee. Embryo fixations and colorimetric *in situ* hybridizations were performed using standard protocols^{7,31}. See Methods for fluorescent *in situ* hybridization (FISH) protocol. Photographs were taken using Zeiss Axiocam MRC5 or MRm cameras on a Zeiss AxioImager.Z1 or a Discovery.V12. Images were acquired using Zeiss Axiovision 4.8 software and adjusted for colour balance and/or levels or gamma using Axiovision 4.8 or Adobe Photoshop CS3 or CS5 software. Images of experimental and control embryos were processed using the same parameters. *S. kowalevskii* homologues of vertebrate genes were identified in an expressed sequence tag (EST) library screen⁴⁷. Amino acid sequences were aligned using ClustalW⁴⁸, and putative homologues were confirmed by constructing gene trees using MrBayes 3.1.2 (refs 49,50) with parameters optimized for each gene (Supplementary Figs 4 and 5). See Supplementary Table 2 for accession numbers.

Full Methods and any associated references are available in the online version of the paper at www.nature.com/nature.

Received 15 November 2011; accepted 6 January 2012.

- Echevarria, D., Vieira, C., Gimeno, L. & Martinez, S. Neuroepithelial secondary organizers and cell fate specification in the developing brain. *Brain Res. Brain Res. Rev.* **43**, 179–191 (2003).
- Wilson, S. W. & Houart, C. Early steps in the development of the forebrain. *Dev. Cell* **6**, 167–181 (2004).
- Wurst, W. & Bally-Cuif, L. Neural plate patterning: upstream and downstream of the isthmic organizer. *Nature Rev. Neurosci.* **2**, 99–108 (2001).
- Wicht, H. & Lacalli, T. C. The nervous system of amphioxus: structure, development, and evolutionary significance. *Can. J. Zool.* **150**, 122–150 (2005).
- Lacalli, T. C. Prospective protochordate homologs of vertebrate midbrain and MHB, with some thoughts on MHB origins. *Int. J. Biol. Sci.* **2**, 104–109 (2006).
- Meinertzhagen, I. A., Lemaire, P. & Okamura, Y. The neurobiology of the ascidian tadpole larva: recent developments in an ancient chordate. *Annu. Rev. Neurosci.* **27**, 453–485 (2004).
- Lowe, C. J. et al. Anteroposterior patterning in hemichordates and the origins of the chordate nervous system. *Cell* **113**, 853–865 (2003).
- Holland, L. Z. & Short, S. Gene duplication, co-option and recruitment during the origin of the vertebrate brain from the invertebrate chordate brain. *Brain Behav. Evol.* **72** (2008).
- Holland, L. Z. Chordate roots of the vertebrate nervous system: expanding the molecular toolkit. *Nature Rev. Neurosci.* **10**, 736–746 (2009).
- Irimia, M. et al. Conserved developmental expression of *Fzef* in chordates and *Drosophila* and the origin of the *Zona Limitans Intrathalamica* (ZLI) brain organizer. *EvoDevo.* **1**, 7 (2010).
- Tomer, R., Denes, A. S., Tessmar-Raible, K. & Arendt, D. Profiling by image registration reveals common origin of annelid mushroom bodies and vertebrate pallium. *Cell* **142**, 800–809 (2010).
- Urbach, R. A procephalic territory in *Drosophila* exhibiting similarities and dissimilarities compared to the vertebrate midbrain/hindbrain boundary region. *Neural Dev.* **2**, 23 (2007).
- Crossley, P. H., Martinez, S. & Martin, G. R. Midbrain development induced by FGFB in the chick embryo. *Nature* **380**, 66–68 (1996).
- Reifers, F. et al. *Fgf8* is mutated in zebrafish acerebellar (*ace*) mutants and is required for maintenance of midbrain-hindbrain boundary development and somitogenesis. *Development* **125**, 2381–2395 (1998).

15. Houart, C. *et al.* Establishment of the telencephalon during gastrulation by local antagonism of Wnt signaling. *Neuron* **35**, 255–265 (2002).
16. Paek, H., Gutin, G. & Hebert, J. M. FGF signaling is strictly required to maintain early telencephalic precursor cell survival. *Development* **136**, 2457–2465 (2009).
17. Kiecker, C. & Lumsden, A. Hedgehog signaling from the ZLI regulates diencephalic regional identity. *Nature Neurosci.* **7**, 1242–1249 (2004).
18. Scholpp, S., Wolf, O., Brand, M. & Lumsden, A. Hedgehog signalling from the zona limitans intrathalamica orchestrates patterning of the zebrafish diencephalon. *Development* **133**, 855–864 (2006).
19. Meulemans, D. & Bronner-Fraser, M. Insights from amphioxus into the evolution of vertebrate cartilage. *PLoS ONE* **2**, e787 (2007).
20. Imai, K. S., Stolfi, A., Levine, M. & Satou, Y. Gene regulatory networks underlying the compartmentalization of the Ciona central nervous system. *Development* **136**, 285–293 (2009).
21. Shimeld, S. M. The evolution of the hedgehog gene family in chordates: insights from amphioxus hedgehog. *Dev. Genes Evol.* **209**, 40–47 (1999).
22. Takatori, N., Satou, Y. & Satoh, N. Expression of hedgehog genes in *Ciona intestinalis* embryos. *Mech. Dev.* **116**, 235–238 (2002).
23. Scholpp, S. & Lumsden, A. Building a bridal chamber: development of the thalamus. *Trends Neurosci.* **33**, 373–380 (2010).
24. Bertrand, S. *et al.* Amphioxus FGF signaling predicts the acquisition of vertebrate morphological traits. *Proc. Natl Acad. Sci. USA* **108**, 9160–9165 (2011).
25. Holland, L. Z., Holland, N. N. & Schubert, M. Developmental expression of *AmphiWnt1*, an amphioxus gene in the *Wnt1*/wingless subfamily. *Dev. Genes Evol.* **210**, 522–524 (2000).
26. Bourlat, S. J. *et al.* Deuterostome phylogeny reveals monophyletic chordates and the new phylum Xenoturbellida. *Nature* **444**, 85–88 (2006).
27. Darras, S., Gerhart, J., Terasaki, M., Kirschner, M. & Lowe, C. J. β -catenin specifies the endomesoderm and defines the posterior organizer of the hemichordate *Saccoglossus kowalevskii*. *Development* **138**, 959–970 (2011).
28. Gillis, J. A., Fritzenwanker, J. H. & Lowe, C. J. A stem-deuterostome origin of the vertebrate pharyngeal transcriptional network. *Proc. R. Soc. B* **279**, 237–246 (2012).
29. Lowe, C. J. *et al.* Dorsoventral patterning in hemichordates: insights into early chordate evolution. *PLoS Biol.* **4**, e291 (2006).
30. Shimamura, K. & Rubenstein, J. L. Inductive interactions direct early regionalization of the mouse forebrain. *Development* **124**, 2709–2718 (1997).
31. Fukuchi-Shimogori, T. & Grove, E. A. Neocortex patterning by the secreted signaling molecule FGF8. *Science* **294**, 1071–1074 (2001).
32. Walshe, J. & Mason, I. Unique and combinatorial functions of *Fgf3* and *Fgf8* during zebrafish forebrain development. *Development* **130**, 4337–4349 (2003).
33. Garel, S., Huffman, K. J. & Rubenstein, J. L. Molecular regionalization of the neocortex is disrupted in *Fgf8* hypomorphic mutants. *Development* **130**, 1903–1914 (2003).
34. Mohammadi, M. *et al.* Structures of the tyrosine kinase domain of fibroblast growth factor receptor in complex with inhibitors. *Science* **276**, 955–960 (1997).
35. Lagutin, O. V. *et al.* Six3 repression of Wnt signaling in the anterior neuroectoderm is essential for vertebrate forebrain development. *Genes Dev.* **17**, 368–379 (2003).
36. Crossley, P. H., Martinez, S., Ohkubo, Y. & Rubenstein, J. L. Coordinate expression of *Fgf8*, *Otx2*, *Bmp4*, and *Shh* in the rostral prosencephalon during development of the telencephalic and optic vesicles. *Neuroscience* **108**, 183–206 (2001).
37. Hébert, J. M. & Fishell, G. The genetics of early telencephalon patterning: some assembly required. *Nature Rev. Neurosci.* **9**, 678–685 (2008).
38. Zeltser, L. M., Larsen, C. W. & Lumsden, A. A new developmental compartment in the forebrain regulated by Lunatic fringe. *Nature Neurosci.* **4**, 683–684 (2001).
39. Scholpp, S. *et al.* *Otx11*, *Otx2* and *Irx1b* establish and position the ZLI in the diencephalon. *Development* **134**, 3167–3176 (2007).
40. Chen, J. K., Taipale, J., Cooper, M. K. & Beachy, P. A. Inhibition of Hedgehog signaling by direct binding of cyclopamine to Smoothened. *Genes Dev.* **16**, 2743–2748 (2002).
41. Simon, H. H., Thuret, S. & Alberi, L. Midbrain dopaminergic neurons: control of their cell fate by the engrailed transcription factors. *Cell Tissue Res.* **318**, 53–61 (2004).
42. McMahon, A. P., Joyner, A. L., Bradley, A. & McMahon, J. A. The midbrain-hindbrain phenotype of *Wnt-1*^{-/-} mice results from stepwise deletion of engrailed-expressing cells by 9.5 days postcoitum. *Cell* **69**, 581–595 (1992).
43. Nomaksteinsky, M. *et al.* Centralization of the deuterostome nervous system predates chordates. *Curr. Biol.* **19**, 1264–1269 (2009).
44. Gavino, M. A., Reddien, P. W. & A. Bmp/Admp regulatory circuit controls maintenance and regeneration of dorsal-ventral polarity in planarians. *Curr. Biol.* **21**, 294–299 (2011).
45. Grande, C. & Patel, N. H. Nodal signalling is involved in left–right asymmetry in snails. *Nature* **457**, 1007–1011 (2009).
46. Campo-Paysaa, F., Marletaz, F., Laudet, V. & Schubert, M. Retinoic acid signaling in development: tissue-specific functions and evolutionary origins. *Genesis* **46**, 640–656 (2008).
47. Freeman, R. M. Jr *et al.* cDNA sequences for transcription factors and signaling proteins of the hemichordate *Saccoglossus kowalevskii*: efficacy of the expressed sequence tag (EST) approach for evolutionary and developmental studies of a new organism. *Biol. Bull.* **214**, 284–302 (2008).
48. Larkin, M. A. *et al.* Clustal W and Clustal X version 2.0. *Bioinformatics* **23**, 2947–2948 (2007).
49. Ronquist, F. & Huelsenbeck, J. P. MrBayes 3: Bayesian phylogenetic inference under mixed models. *Bioinformatics* **19**, 1572–1574 (2003).
50. Huelsenbeck, J. P. & Ronquist, F. MRBAYES: Bayesian inference of phylogenetic trees. *Bioinformatics* **17**, 754–755 (2001).

Supplementary Information is linked to the online version of the paper at www.nature.com/nature.

Acknowledgements We thank J. Gerhart and M. Kirschner for assistance and support, R. Freeman for bioinformatics assistance, E. Farrelly, M. Terasaki and S. Darras for technical guidance, the members of the Lowe laboratory for discussions, and G. Wray and J. Gerhart for comments on drafts of the manuscript. We also thank the staff of the Marine Biological Laboratory, the Waquoit Bay National Estuarine Research Reserve, Carl Zeiss and Nikon for assistance during our field season. This work was funded by the Searle Kinship Foundation, Brain Research Foundation and National Science Foundation grant 1049106 (C.J.L.), National Institutes of Health grant R01 HD42330 (E.A.G.) and the University of Chicago Hinds Fund (A.M.P.). A.M.P. was supported by a Marine Biological Laboratory Frank R. Lillie Fellowship, National Institute of Child Health and Development institutional training grant 1T32HD055164-01A1, and National Institute of Neurological Disorders and Stroke pre-doctoral fellowship 1F31NS074738-01A1. J.A. was supported by a National Science and Engineering Research Council of Canada pre-doctoral grant.

Author Contributions A.M.P., C.J.L. and J.A. conceived the project. A.M.P. and C.J.L. performed the hemichordate experiments and wrote the paper. E.E.M. and S.A. performed mouse experiments, and E.A.G. edited the paper. All authors discussed and commented on the data.

Author Information *S. kowalevskii* gene sequences have been deposited in GenBank, and accession numbers are provided in Supplementary Table 2. Reprints and permissions information is available at www.nature.com/reprints. The authors declare no competing financial interests. Readers are welcome to comment on the online version of this article at www.nature.com/nature. Correspondence and requests for materials should be addressed to C.J.L. (clowe@stanford.edu).

METHODS

Embryo procurement. Gravid *S. kowalevskii* adults were collected from the intertidal zone of sandy estuaries near Woods Hole, Massachusetts, and maintained in flow-through seawater tables at the Woods Hole Marine Biological Laboratory. Spawning and embryo rearing were carried out using established techniques⁷. Mouse embryos were obtained using standard protocols approved by the University of Chicago Institutional Animal Care and Use Committee.

Experimental manipulations. SU5402 (Calbiochem) and cyclopamine (Calbiochem) were resuspended in minimal volumes of DMSO and diluted in 0.2 μ m-filtered sea water for treatments. Embryos were raised at room temperature. Control embryos were obtained from the same batches and raised in an equivalent concentration of DMSO. siRNA microinjections were performed as described previously^{27,29}. siRNAs were resuspended at 100 mM and injected at 1/10 concentration in a suspension buffer²⁷ including either calcein or lysinated 10,000 MW tetramethylrhodamine dextran (Molecular Probes). Unsuccessfully injected embryos, or embryos with abnormal cleavage patterns, were discarded. siRNAs were ordered from Ambion or Qiagen, and sequences are provided in Supplementary Table 1.

In situ hybridizations. Colorimetric *in situ* hybridizations were performed as described previously^{7,31}. Clonal descendants of injected blastomeres were identified after *in situ* hybridization using anti-tetramethylrhodamine (Molecular Probes) immunofluorescence. For FISH, pre-hybridization steps were performed using our standard protocol. For double FISH, embryos were simultaneously hybridized with antisense RNA probes for both genes labelled separately with digoxigenin-11-UTP (Roche) or fluorescein-12-UTP (Roche). Owing to a reduced sensitivity of FISH, we typically used two to three times more probe compared to colorimetric methods. We used our standard protocol for post-hybridization washes and blocking steps. Embryos were then incubated in anti-digoxigenin-POD or anti-fluorescein-POD antibodies (Roche) diluted 1:200 in blocking solution (2% Roche blocking reagent, 1 \times MAB) for 4 h at room temperature on a rotary shaker. Embryos were washed four times in 1 \times MAB for 30 min and once for 1 h at room temperature, or overnight at 4 $^{\circ}$ C. Embryos were then washed in 0.1 M imidazole (Sigma) in 1 \times PBS for 10 min at room temperature and probes were detected using a Tyramide Signal Amplification (TSA) Plus

kit (Perkin-Elmer). Embryos were rinsed in 1 \times amplification diluent and incubated in cyanine-3 or cyanine-5 tyramide diluted 1:50 in 1 \times amplification diluent for 45 min on a rotary shaker at room temperature. Embryos were washed three times in detergent solution (1% triton X-100, 1% SDS, 0.5% sodium deoxycholate, 50 mM Tris-HCl pH 8.0, 1 mM EDTA pH 8.0, 150 mM sodium chloride) for 20 min at 60 $^{\circ}$ C. When detecting a second gene, we washed the embryos once for 20 min in solution X (50% formamide, 2 \times SSC and 1% SDS) at 60 $^{\circ}$ C. Embryos were then washed three times in 1 \times MAB for 5 min and returned to the blocking step.

For genes with low signal under standard FISH methods, we performed an additional 2,4-dinitrophenol (DNP) amplification step. After primary antibody incubation and 1 \times MAB washes, embryos were incubated in DNP amplification reagent that was diluted 1:50 in 1 \times amplification diluent (Perkin-Elmer) for 5–10 min at room temperature on a rotary shaker. Embryos were washed four times in 1 \times MAB for 30 min and once for 1 h at room temperature, re-blocked for 1 h and incubated in anti-DNP-HRP antibody (Perkin-Elmer) that was diluted 1:200 in blocking solution for 4 h at room temperature on a rotary shaker. Embryos were washed four times in 1 \times MAB for 30 min and once for 1 h at room temperature. Expression was then detected using a TSA Plus kit (Perkin-Elmer) as described above.

Photography. Embryos were photographed using Zeiss Axiocam MRc5 or MRm cameras on Zeiss AxioImager.Z1 or Discovery.V12 microscopes. For optical clearing, *S. kowalevskii* embryos were dehydrated into methanol, cleared using Murray's clearing reagent (1:2 benzyl alcohol to benzyl benzoate) and mounted in permount (Fisher Scientific). Cleared embryos were imaged under differential interference contrast optics and uncleared embryos were photographed in 1 \times PBS or 1 \times MAB on agarose-coated dishes. Images were acquired using Zeiss Axiovision 4.8 software and adjusted for colour balance and/or levels or gamma using Zeiss Axiovision 4.8 or Adobe Photoshop CS3 or CS5 software. Images of experimental and control embryos were processed using the same parameters.

Gene identification. *S. kowalevskii* homologues of vertebrate genes were identified in an EST library screen⁴⁷, amino acid sequences were aligned using ClustalW⁴⁸ and putative homologues were confirmed by constructing gene trees using MrBayes 3.1.2 (refs 49,50) with parameters optimized for each gene (Supplementary Figs 4 and 5). See Supplementary Table 2 for accession numbers.